

Figure S1. *Chlamydia* infection alters the Tyr phosphoproteome of epithelial cells, Related to Figure 2.

(A-B) TepP prominently increased the levels of tyrosine phosphorylation of the actin-binding proteins EPS8 and EPS8L2. (A) Volcano plot comparing the pTyr phospho-proteome of A2EN cells infected with a *tepP* mutant complemented with pTepP compared to the uninfected (“mock”) control. (B) Bar graphs depicts the GO enrichment analysis of biological processes associated with TepP-expressing *Chlamydia*.

(C-D) TepP-independent changes to the host Tyr phosphoproteome upon infection with *Chlamydia*. (C) Volcano plot comparing the pTyr phospho-proteome of A2EN cells infected with *tepP* mutants transformed with an empty expression plasmid (“pVector”) to the mock control. (D) Bar graphs depicts the TepP-independent GO enrichment analysis of biological processes.

Figure S2. TepP associates with EPS8 in an actin- and Tyr phosphorylation-independent manner, Related to Figures 2 and 3.

(A-B) *EPS8* associates with *TepP* in an actin-independent manner. (A) Confocal images of MEF cells stably expressing EGFP-EPS8 (green) and transfected either mCh or mCh-TepP (magenta) treated with DMSO or Latrunculin A for 1 h and stained for DNA (blue). (B) Fluorescence images of HeLa cells transfected with full-length EGFP-EPS8 (green) or EPS8 deletion constructs alone or with mCh-TepP (magenta).

(C-D) *Src/Yes/Fyn (SYF)* activities are not required for *EPS8* recruitment to nascent inclusions. (C) Confocal images of MEF cells or SYF (+/- *Src*) cells infected for 1 h with CTL2 and immunostained for Slc1 (green) and EPS8 (magenta). (D) Quantification of the percent EPS8-positive inclusions per cell (n = 12-18 cells; unpaired, two-tailed t-test).

(E-G) Mutagenesis of the four Tyr residues to Phe in EPS8 does not impact its recruitment to nascent inclusions or its colocalization with mCh-TepP. (E) Fluorescence images of HeLa cells expressing EGFP-EPS8 and EGFP-EPS8-4xYF (magenta) and infected with mCherry-expressing CTL2 (green) for 1 h. (F) Quantification of EPS8-positive inclusions per cell (n = 35-39 cells; unpaired, two-tailed t-test). (G) Fluorescence images of HeLa cells transfected with EGFP-EPS8-4xYF (green) and mCh or mCh-TepP (magenta) expression construct.

(H) *Src* inhibitors decrease *EPS8* expression and phosphorylation. Whole cells lysates from HeLa cells incubated with *Src* family kinase inhibitors and either uninfected or infected with CTL2 were subjected to western blot analysis for pTyr (pY), EPS8, α -tubulin, and HtrA.

(D, F). Scatter plots represent individual cells and the line denotes the median.

Figure S3. TepP and EPS8 promote the disruption of adherens junctions during early infection, Related to Figure 4.

(A-C) *A2EN^{Cas9} EPS8 KO cells exhibit normal formation of adherens junctions that are recalcitrant to disruption during early Chlamydia infection.* (A) Confocal images of A2EN^{Cas9} and A2EN^{Cas9} EPS8 KO cells cultured on collagen-coated filters and stained for F-actin (magenta), and DNA (blue), and either (A) E-cadherin (green, white) or (B) Afadin (green, white). (C) Fluorescence images of A2EN^{Cas9} and A2EN^{Cas9} EPS8 KO cells infected with CTL2-GFP (green) for 1 h and stained for E-cadherin (magenta, white) and DNA (blue).

(D) *TepP promotes the disruption of adherens junctions during early infection.* Confocal images of A2EN cells infected with CTL2 or *tepP* mutant bacteria for 2 h and immunostained for MOMP (white), β -catenin (green) and F-actin (magenta).

(E-F) *Temporal loss of ZO-1 at early inclusion is followed by tight junction repair.* (E) Fluorescence images of ZO-1 (magenta) at the indicated time points with respect to CTL2-GFP (green) inclusions. (F) Quantification of ZO-1-positive inclusions (n = 15 cells). Box and Whisker plots represent the median and interquartile range and +/- either the min or max values or 1.5*IQR.

Figure S4. Cell polarity and morphometric analysis of *Eps8* ^{+/+} and *Eps8* ^{-/-} organoids, Related to

Figure 5. (A) Representative brightfield images of *Eps8*^{+/+} and *Eps8*^{-/-} endometrial organoids in culture for seven days. (B) Fluorescence images of *Eps8*^{+/+} and *Eps8*^{-/-} endometrial organoids stained for EPS8 (green), F-actin (magenta) and DNA (blue). (C) Quantification of organoid size (n = 75-77 organoids; unpaired, two-tailed t-test). Box and Whisker plots represent the median +/- 1.5*IQR (D) Confocal images of *Eps8*^{+/+} and *Eps8*^{-/-} organoids stained for β -catenin (green), F-actin (magenta), and DNA (blue). (E) Quantification of cell height in *Eps8*^{+/+} and *Eps8*^{-/-} organoids (n = 51 cells; unpaired, two-tailed t-test). Box and Whisker plots represent the media and interquartile range +/- either the min or max values or 1.5*IQR.

Figure S5. TepP expression is sufficient to disrupt epithelial tight junctions, Related to Figure 6.

(A-D) *TepP alters the localization of EPS8 and ZO-1 in polarized MDCK cells.* (A) Confocal images of polarized MDCK cells expressing with mCh or mCh-TepP (magenta) and immunostained for EPS8 (green) and DNA (blue). (B) Quantification of EPS8 fluorescence intensity at the lateral membrane (n = 28 measurements; unpaired, two-tailed t-test). (C) Confocal images of polarized MDCK cells expressing mCh or mCh-TepP (magenta) and immunostained for ZO-1 (green) and DNA (blue). Arrows point to regions of tight junction disruption. (D) Quantification of ZO-1 intensity at the lateral membrane (n = 42 measurements; unpaired, two-tailed t-test).

(E) *TepP* and *EPS8* co-localize at sites of tight junction remodeling. Fluorescence images of polarized MDCK cells expressing mCh-TepP (magenta) and immunostained for *EPS8* (cyan), ZO-1 (green), and DNA (white). Arrow denotes TepP and *EPS8* at a site of ZO-1 remodeling.

(F-G) *TepP* delays MDCK polarization and reduces TEER. (F) Brightfield and fluorescence images of polarizing MDCK cells transfected mCh or mCh-TepP (magenta) for two days. Enlarged area scale bars, 100 μ m. (G) TEER was measured every 24 h for three days in polarizing MDCK cells either untreated (“mock”) or after transfection with mCh or mCh-TepP (n = 3 independent replicates). Data are represented as the mean \pm SD.

(B, D) Scatter plots represent individual fluorescence measurements and the line denotes the median.

*** p < 0.001

Figure S6. Generation and characterization of a *C. muridarum tepP* mutant, Related to Figure 7.

(A) *TargeTron* mediated disruption of *tepP*. PCR analysis of *C. muridarum* wild-type and *tepP* mutant DNA targeting full-length *tepP* (TC0268), *bla*, and the *TargeTron* insertion site.

(B-C) *C. muridarum* TepP promotes *EPS8* recruitment to nascent inclusions. (B) Fluorescence images of A2EN cells infected with *C. muridarum* wild-type or *tepP* mutant bacteria for 1 h and immunostained for *EPS8* (green), F-actin (magenta), and DNA (blue). (C) Quantification of *EPS8*-positive inclusions. Scatter plots represent individual cells and the line denotes the median (n = 30 cells; unpaired, two-tailed t-test).

(D-E) The *C. muridarum* TepP promotes A2EN dispersion. (D) Fluorescence images of polarized A2EN cells infected with *C. muridarum* wild-type or *tepP* mutant bacteria for 1 h and stained for F-actin (white) and DNA (blue). (E) Quantification of cell-free area. Scatter plot represents individual fields of view and the line denotes the median (n = 30 fields of view; unpaired, two-tailed t-test).

(F-G) *C. muridarum tepP* mutants are defective in ascension from the lower genital tract and induce lower pathology. (F) Mice were infected transcervically with *C. muridarum* wild-type or *tepP* mutant bacteria and swabbed at the indicated day. The number of recoverable IFU were quantified and plotted (n = 5 mice). Note that these mice are from a replicate in Fig 7I but the infection was allowed to progress for 45 d. (G) Representative images of the genital tract infected with *C. muridarum* wild-type and *tepP* mutant bacteria at 45 d. Gross pathology, including hydrosalpinx and hydrometra, were quantified.

*** p < 0.001

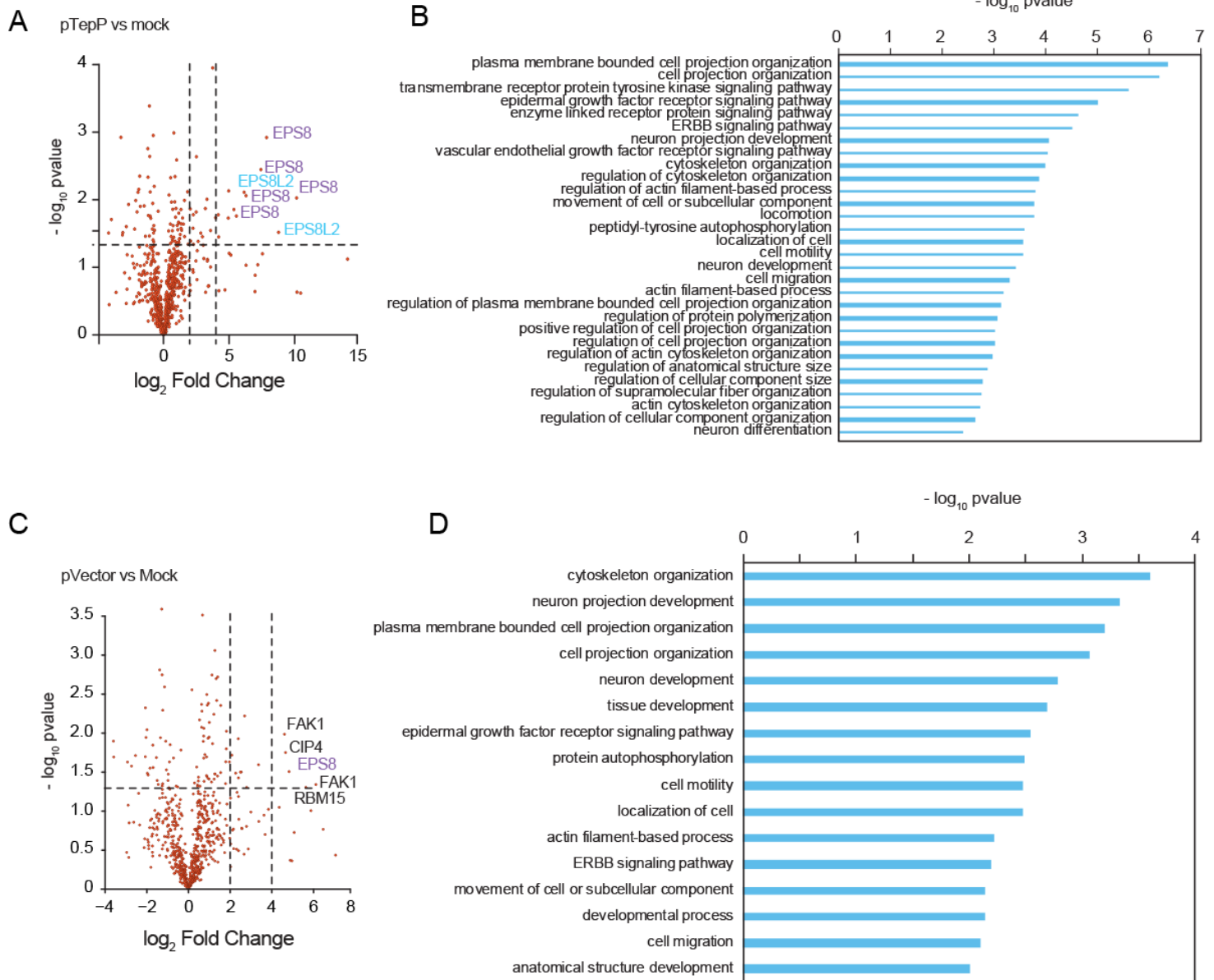


Figure S1 (Dolat et al.)

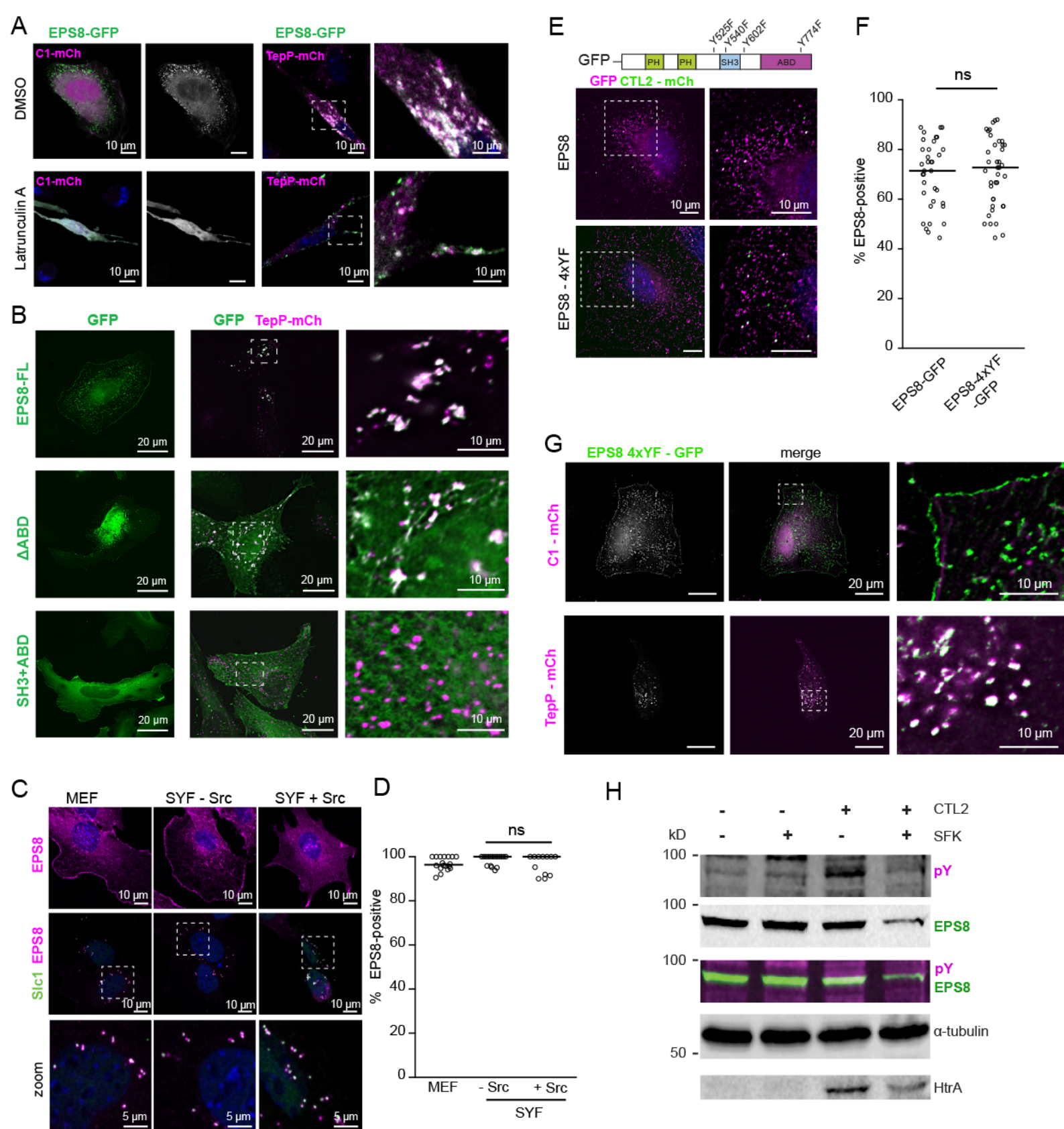


Figure S2 (Dolat et al.)

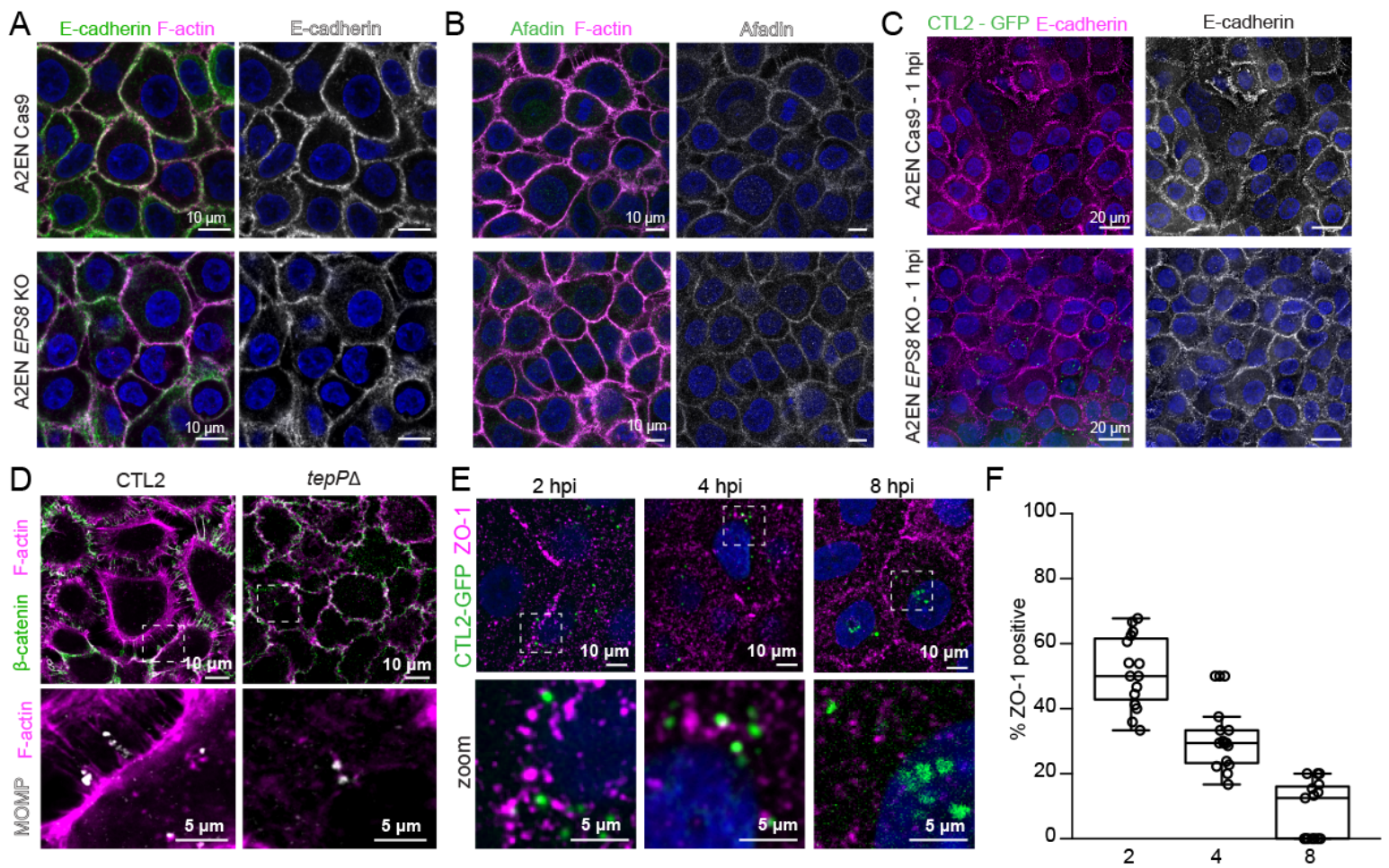


Figure S3 (Dolat et al.)

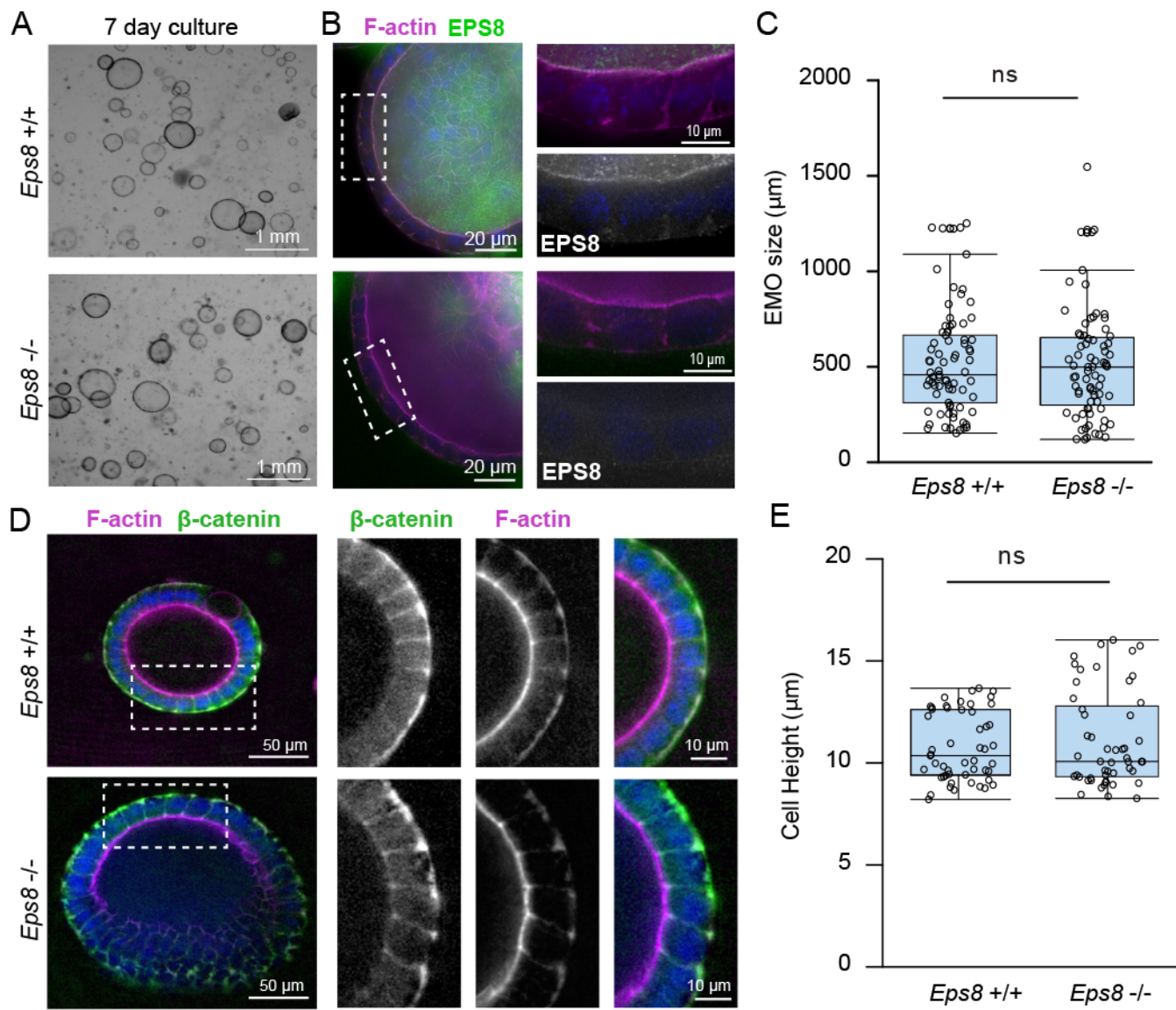


Figure S4 (Dolat et al.)

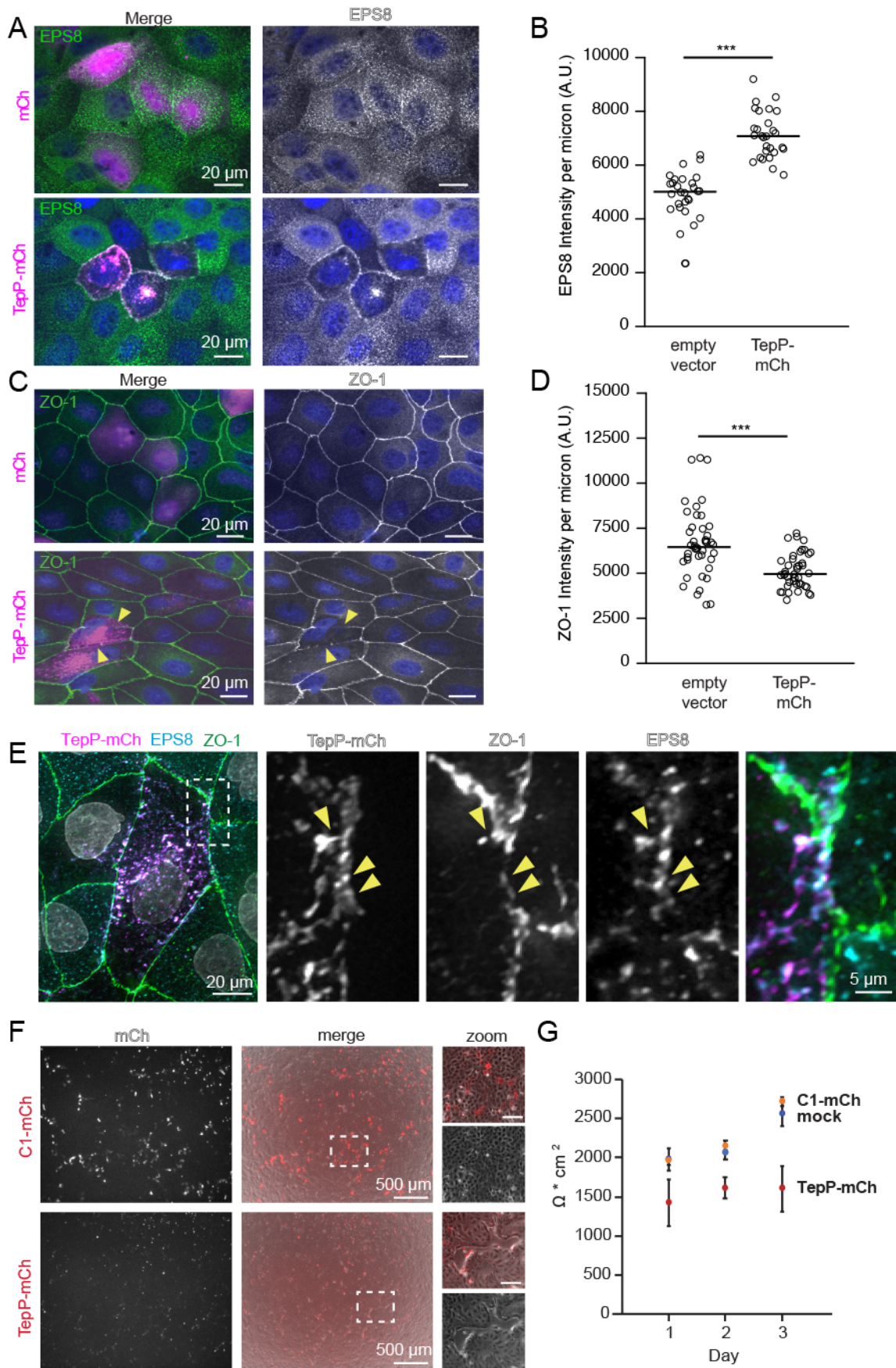


Figure S5 (Dolat et al.)

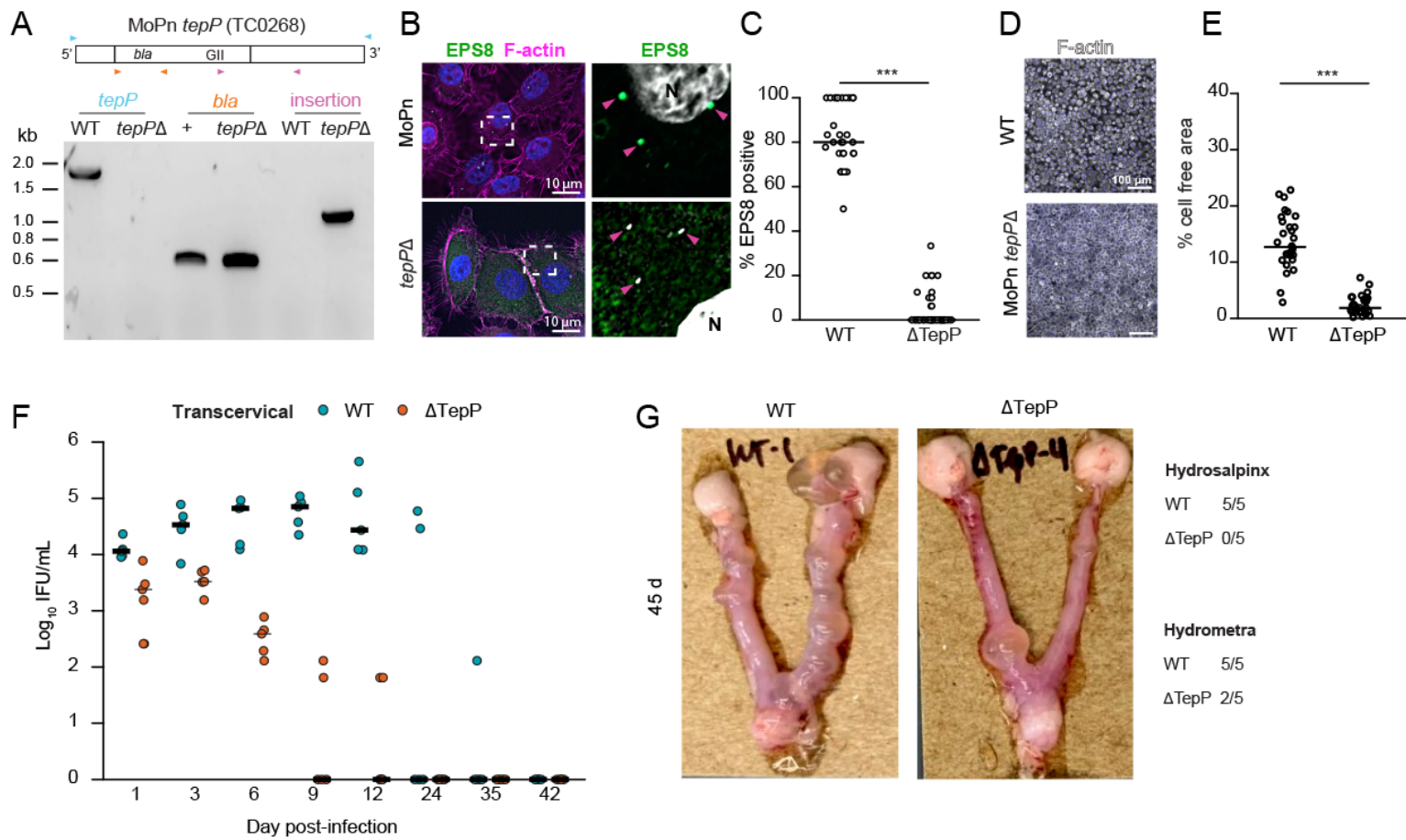


Figure S6 (Dolat et al.)

Table S2. List of oligonucleotides used in this study, Related to STAR Methods.

Purpose	5' → 3'
mCherry-TepP	TCTCGAGCTCAAATGAGCATCGGGGAGTACG CGGTGGATCCTTATTCCTATCGACTTCTCTATC
EPS8 4x Y→F	Y525 TGTTTTGAGTGGTTCAAATTTCTATCTATATGGCGATTAGAAGTTGG Y525 CCAACTTCTAATCGCCATATAGATAGAAATTTGAACCACTCAAACA Y540 CCTTGCTACAAAGTCAAAGTTGGATTTGGCATATTTCTTGG Y540 CCAAGAAATATGCCAAATCCAAGTTTGACTTTGTAGCAAGG Y602 TCTGTATAGTATGAGTAAAAGGTGGATCAGCACGCC Y602 GCGGTGCTGATCCACCTTTACTCATACTATACAGA Y774 GTACAGTGATTTGGCTAAAGACTCTCGCCCCCTCA Y774 TGAAGGGGCGAGAGTCTTTAGCCAAATCACTGTAC
EGFP-EPS8-ΔABD	TCTCGAGCTCAAGCTATGAATGGTCATATTTCTAATCATCCC CCGCGGTACCGTCGATTATGACACAGGAACAGGTGCTG
EGFP-EPS8-SH3+ABD	TCTCGAGCTCAAGCTATGCAACCCAAGAAATATGCCAAATC CCGCGGTACCGTCGATTAGTGACTGCTTCCTTCATCA
Retargeting pDFTT3 to CTL0063 (<i>tmeA</i>)	IBS1/2 AAAAAAGCTTATAATTATCCTTACTCAACCTATTGGTGCGCCAGATAGGGTG EBS1/delta CAGATTGTACAAATGTGGTGATAACAGATAAGTCCTATTGTCTAACTTACCTTTCTTTGT EBS2 TGAACGCAAGTTTCTAATTTTCGGTTTTGAGTCGATAGAGGAAAGTGTCT
Retargeting pDFTT3 to CTL0064 (<i>tmeB</i>)	IBS1/2 AAAAAAGCTTATAATTATCCTTACTTCACTGACCCGTGCGCCAGATAGGGTG EBS1/delta CAGATTGTACAAATGTGGTGATAACAGATAAGTCTGACCCCTTAACTTACCTTTCTTTGT EBS2 TGAACGCAAGTTTCTAATTTTCGGTTTTGAAGTCGATAGAGGAAAGTGTCT
Retargeting pDFTT3 to TC0268 (<i>tepP</i>)	IBS1/2 AAAAAAGCTTATAATTATCCTTAGCTACCGCTACGTGCGCCAGATAGGGTG EBS1/delta CAGATTGTACAAATGTGGTGATAACAGATAAGTCGCCTACTCTAACTTACCTTTCTTTGT EBS2 TGAACGCAAGTTTCTAATTTTCGATTGTAGCTCGATAGAGGAAAGTGTCT
EBS Universal	CGAAATTAGAACTTGCGTTTCAGTAAAC
CTL0063 forward	ATGAGTATTCGACCTAC
CTL0064 reverse	ACTTCGAACACGCAATGCATC
<i>C.mu tepP</i> forward	GGTACCCGTCGTGTTGTCTAAGTCTC
<i>C.mu tepP</i> reverse	GCGGCCGCTTATTGATTATCTAGTTCC
<i>C.mu tepP</i> junction	ACTACCTGTATCAACCTCTGATAG
aadA FOR	GTAACGCGTCCCGGGCCTGATAGTTGGCTGTGAG
aadA REV	TCTACGCGTTGCCTGACGATGCGTGAG
bla FOR	CGATCTGTCTATTTTCGTTCA
bla REV	CGGTATTATCCCGTATTGAC
Human <i>EPS8</i> gRNA	TCATCTCTCCAGTGTGATG
<i>Eps8</i> exon 4 sgRNA 3	CTGAGTTTCGTTACCTACTATGG
<i>Eps8</i> exon 4 sgRNA 4	TTACTGTTCAAGCGCTTAACTGG

<i>Eps8</i> exon 4 FOR	TTTATTCTACTATAGCTGACGTC
<i>Eps8</i> exon 4 REV	TAGAGGGAGGAGGATTCATAGTTC
CTL2 16s rRNA FOR	GGAGGCTGCAGTCGAGAATCT
CLT2 16s rRNA REV	TTACAACCCTAGAGCCTTCATCACA
Mouse <i>Gapdh</i> FOR	ACTGAGCAAGAGAGGCCCTA
Mouse <i>Gapdh</i> REV	TATGGGGGTCTGGGATGGAA